EARTHQUAKE ENGINEERING AND STRUCTURAL DYNAMICS
Earthquake Engng Struct. Dyn. 2008; **37**:1333–1348
Published online 21 April 2008 in Wiley InterScience (www.interscience.wiley.com). DOI: 10.1002/eqe.820

Wavelet-based simulation of spectrum-compatible aftershock accelerograms

S. Das and V. K. Gupta*, †

Department of Civil Engineering, Indian Institute of Technology Kanpur, Kanpur 208016, India

SUMMARY

In damage-based seismic design it is desirable to account for the ability of aftershocks to cause further damage to an already damaged structure due to the main shock. Availability of recorded or simulated aftershock accelerograms is a critical component in the non-linear time-history analyses required for this purpose, and simulation of realistic accelerograms is therefore going to be the need of the profession for a long time to come. This paper attempts wavelet-based simulation of aftershock accelerograms for two scenarios. In the first scenario, recorded main shock and aftershock accelerograms are available along with the pseudo-spectral acceleration (PSA) spectrum of the anticipated main shock motion, and an accelerogram has been simulated for the anticipated aftershock motion such that it incorporates temporal features of the recorded aftershock accelerogram. In the second scenario, a recorded main shock accelerogram is available along with the PSA spectrum of the anticipated main shock motion and PSA spectrum and strong motion duration of the anticipated aftershock motion. Here, the accelerogram for the anticipated aftershock motion has been simulated assuming that temporal features of the main shock accelerogram are replicated in the aftershock accelerograms at the same site. The proposed algorithms have been illustrated with the help of the main shock and aftershock accelerograms recorded for the 1999 Chi–Chi earthquake. It has been shown that the proposed algorithm for the second scenario leads to useful results even when the main shock and aftershock accelerograms do not share the same temporal features, as long as strong motion duration of the anticipated aftershock motion is properly estimated. Copyright © 2008 John Wiley & Sons, Ltd.

Received 8 November 2007; Revised 9 March 2008; Accepted 12 March 2008

KEY WORDS: damage-based design; wavelet transform; aftershocks; synthetic accelerogram

1. INTRODUCTION

The existing earthquake design philosophy does not envisage any role of aftershocks assuming that those are too weak to cause further damage to an already damaged structure during the main

*Correspondence to: V. K. Gupta, Department of Civil Engineering, Indian Institute of Technology Kanpur, Kanpur 208016, India.
†E-mail: vinaykg@iitk.ac.in

shock. This assumption is not always true, particularly when the main shock causes significant degradation in the stiffness and/or strength of the structure and the aftershocks are too strong for the weakened structure. In this situation, even though the structure survives the main shock, it may collapse during one of the aftershocks. It may be noted that aftershocks occur soon after the main shock and thus it is impractical to repair the damaged structure before the occurrence of the aftershocks. Therefore, as shown by Gupta *et al.* [1], the yield design levels may have to be raised to account for aftershocks, particularly when the arrival of energy during the main shock takes place over a shorter duration.

A proper evaluation of the seismic performance of a structure during a main shock and following aftershocks would require time-history analyses by using the accelerograms corresponding to the main shock and first few aftershocks. These accelerograms should be compatible with the (design) main shock motion anticipated at the site and in keeping with the present practice of seismic hazard characterization, compatibility with the pseudo-spectral acceleration (PSA) spectrum representing such an action becomes desirable [2]. Availability of the recorded accelerograms for aftershocks is severely limited at this stage, and even when those are available, their compatibility with the design main shock motion is not guaranteed. It is therefore necessary to simulate aftershock accelerograms that are compatible with the PSA spectrum of the anticipated main shock motion, and no simulation technique seems to have been developed till date to address this long-standing need of the profession.

An attempt is made in this paper to simulate an accelerogram for an anticipated aftershock motion at a site conditional to the anticipated main shock motion at the same site. It is therefore assumed that the PSA spectrum and the time–frequency characteristics of the anticipated main shock motion are available. Further, some information is assumed to be available about the anticipated aftershock motion, either in the form of its time–frequency characteristics or in the form of its PSA spectrum and strong motion duration. Algorithms are thus developed for the following two specific situations, depending on what kind of information is available about the anticipated aftershock motion. In one, the aftershock accelerogram is simulated to possess the given time–frequency characteristics, specified via a recorded aftershock accelerogram, such that it is consistent with the given PSA spectrum of the anticipated main shock motion. It is assumed that the main shock accelerogram is also available for the same site as the recorded aftershock accelerogram. In the second situation, the PSA spectrum and strong motion duration of the anticipated aftershock motion are known instead of its time–frequency characteristics. In the case of main shocks, these two parameters may be estimated in terms of the seismological parameters such as magnitude and epicentral distance (e.g. [3–6]), and it is therefore expected that similar models will be available in the time to come for the aftershocks as well. For the purpose of this paper, these are treated as the input parameters to be provided by the user. The algorithms proposed for both situations are illustrated with the help of the main shock and aftershock records of 1999 Chi–Chi earthquake (magnitude $M_L = 7.3$, focal depth $h = 10.33$ km).

The algorithms proposed in this paper are based on the use of the wavelet transform; hence, a brief review of the wavelet transform as used in the paper is given first for the sake of completeness.

2. REVIEW OF THE WAVELET TRANSFORM

Let $f(t)$ be a function belonging to $L^2(R)$—a space of all finite energy functions. This can be decomposed into wavelet coefficients and reconstructed back from those by using the wavelet

DOI: 10.1002/eqe

transformation and the inverse wavelet transformation, respectively. The continuous wavelet transformation of $f(t)$ is defined with respect to a basis function, $\psi(t)$, as

$$W_\psi f(a,b) = \langle f, \psi_{a,b} \rangle = \int_{-\infty}^{\infty} f(t) \bar{\psi}_{a,b}(t)\, \mathrm{d}t, \quad a, b \in \Re \tag{1}$$

with $\bar{\psi}(t)$ being the complex conjugate of

$$\psi_{a,b}(t) = \frac{1}{|a|^{1/2}} \psi\left(\frac{t-b}{a}\right) \tag{2}$$

Here, a is a scale parameter that controls the frequency content of the dilated basis function and b is the shift parameter that localizes the basis function at and around $t=b$. The function $f(t)$ can be reconstructed back from the wavelet coefficients, $W_\psi f(a,b)$, as

$$f(t) = \frac{1}{2\pi C_\psi} \int_{-\infty}^{\infty} \int_{-\infty}^{\infty} \frac{1}{a^2} W_\psi f(a,b) \psi_{a,b}(t)\, \mathrm{d}a\, \mathrm{d}b \tag{3}$$

with

$$C_\psi = \int_{-\infty}^{\infty} \frac{|\hat{\psi}(\omega)|^2}{|\omega|}\, \mathrm{d}\omega < \infty \tag{4}$$

In Equation (4), $\hat{\psi}(\omega)$ is the Fourier transform of the basis function, $\psi(t)$, defined as

$$\hat{\psi}(\omega) = \frac{1}{\sqrt{2\pi}} \int_{-\infty}^{\infty} \psi(t) \mathrm{e}^{-\mathrm{i}\omega t}\, \mathrm{d}t \tag{5}$$

For the present study, the modified L-P wavelet basis as proposed by Basu and Gupta [7] is used. This is represented as

$$\psi(t) = \frac{1}{\pi\sqrt{\sigma - 1}} \frac{\sin(\sigma\pi t) - \sin(\pi t)}{t} \tag{6}$$

with σ taken as $2^{1/4}$. For $\sigma = 2$, this basis becomes the same as the L-P basis [8] with poorer frequency localization and improved time localization. On discretizing and taking a_j $(=\sigma^j)$ and $b_i = (i-1)\Delta b$ as the discretized values of a and b, respectively [7], $f(t)$ can be reconstructed from its wavelet coefficients as

$$f(t) = \sum_j f_j(t) \tag{7}$$

with

$$f_j(t) = \frac{K \Delta b}{a_j} \sum_i W_\psi f(a_j, b_i) \psi_{a_j, b_i}(t) \tag{8}$$

and

$$K = \frac{1}{4\pi C_\psi} \left(\sigma - \frac{1}{\sigma}\right) \tag{9}$$

DOI: 10.1002/eqe

Here, Δb is taken as 0.02 s. Further, the decomposed time history $f_j(t)$ has energy in the period band, $(2a_j/\sigma, 2a_j)$. Thus, if a total number of 32 decomposed time histories are considered with $j=-21$ to 10, $f(t)$ would span over the period band, 0.044–11.32 s, which is deemed to be sufficient for most earthquake accelerograms.

3. SYNTHESIS WITH RECORDED AFTERSHOCK MOTION

For the algorithm developed in this section, a pair of main shock and aftershock accelerograms recorded at the same site is assumed to be available such that those have similar temporal features as desired in the motions to be simulated. The PSA spectrum for the main shock that will precede the aftershock motion to be simulated is also assumed to be available. The idea here is that we modify the recorded aftershock accelerogram, without disturbing the temporal variations of different frequency waves, such that the modified motion becomes consistent with the PSA spectrum of the anticipated main shock and the recorded main shock motion. There are two wavelet-based methods in which such a modification appears possible.

In the first method (Method I), it is assumed that the PSA spectrum of the aftershock motion to be simulated enjoys the same relationship with the given PSA spectrum of the anticipated main shock as that by the PSA spectrum of the recorded aftershock motion (with the PSA spectrum of the recorded main shock motion). In other words, the period-dependent main-shock-to-aftershock attenuation in PSA spectrum is assumed to remain invariant from event to event. This appears reasonable if the recorded motions are carefully chosen to accurately reflect the characteristics expected in the design motions. Thus, if $\mathrm{PSA}_{\mathrm{Main}}(T)$ is the smoothed PSA spectrum of the given main shock accelerogram and $\mathrm{PSA}_{\mathrm{Aft}}(T)$ is the smoothed PSA spectrum of the given aftershock accelerogram, a non-dimensional factor

$$\alpha(T)=\frac{\mathrm{PSA}_{\mathrm{Aft}}(T)}{\mathrm{PSA}_{\mathrm{Main}}(T)} \tag{10}$$

would describe the period-dependent attenuation from the main shock motion to the aftershock motion. Thus, the PSA spectrum of the anticipated aftershock can be estimated as

$$\mathrm{DS}_{\mathrm{Aft}}(T)=\alpha(T)\mathrm{DS}_{\mathrm{Main}}(T) \tag{11}$$

where $\mathrm{DS}_{\mathrm{Main}}(T)$ is the (design) PSA spectrum for the anticipated main shock. The recorded accelerogram of the aftershock may now be modified so as to be compatible with $\mathrm{DS}_{\mathrm{Aft}}(T)$, following the (wavelet-based) procedure of Mukherjee and Gupta [9]. This procedure preserves the temporal features of the recorded accelerogram in different frequency bands and works well for any combination of the target spectrum and the PSA spectrum of the recorded accelerogram. It may be noted that Method I depends significantly on the correct estimation of $\mathrm{DS}_{\mathrm{Main}}(T)$. At very long periods, both $\mathrm{PSA}_{\mathrm{Main}}(T)$ and $\mathrm{PSA}_{\mathrm{Aft}}(T)$ approach zero values and therefore $\alpha(T)$ may not be reliably estimated. As a result, the modified accelerogram may become unrealistic in the contribution of very long periods.

For the other method (Method II), it will be desirable to recall the procedure of Mukherjee and Gupta [9]. In this procedure, the recorded accelerogram $f(t)$ is decomposed into 32 time histories, $f_j(t)$, $j=-21,-20,\ldots,10$ spanning over the period bands, 0.044–0.053, 0.053–0.063, …, 9.52–11.32 s, respectively. Each of these time histories is now uniformly scaled by a suitable

DOI: 10.1002/eqe

scaling factor, β_j, so that the accelerogram

$$\bar{f}(t) = \sum_{j=-21}^{10} \beta_j f_j(t) \tag{12}$$

becomes compatible with the given PSA spectrum. The factors, β_j, $j = -21, -20, \ldots, 10$ are obtained iteratively. In Method II, it is proposed to obtain the scaling factors that would modify the recorded main shock accelerogram so as to be compatible with the PSA spectrum of the anticipated main shock motion, and to use those factors in Equation (12) for modifying the recorded aftershock accelerogram (taken as $f(t)$).

It may be noted that the scaling factor β_j denotes the factor by which the contribution of the frequency band corresponding to the scale parameter a_j to the recorded motion is scaled up/down for consistency of the modified motion with the target PSA spectrum. This factor is a true indicator of the change in energy levels between the parent motion and the target motion only at higher values of j. Owing to sensitivity of the PSA value (of the target motion) at a period to the β_j's corresponding to the bands of longer periods, the β_j values for lower j's undergo greater adjustments (than those demanded by the actual differences in the energy levels) in the procedure of Mukherjee and Gupta [9] and thus are more fictitious than those for the greater j's. By assuming identical scaling factors for the main shock and aftershock motions, Method II is likely to lead to aftershock accelerograms with unrealistic PSA values at shorter periods. At longer periods, however, β_j becomes almost the same as the ratio, $\mathrm{DS}_{\mathrm{Main}}(T)/\mathrm{PSA}_{\mathrm{Main}}(T)$, and then, both Methods I and II would lead to the aftershock accelerograms with very similar PSA spectra.

For the numerical illustration of Methods I and II proposed above, Aftershock 2352 (occurrence at 23:52 h on September 25, 1999; $M_L = 6.8$) of the Chi–Chi 1999 earthquake recorded at Station N042 along the EW direction is modified for consistency of the main shock motion with the 5% damping USNRC [10] spectrum with zero-period acceleration as $1.0g$. Figure 1 shows the comparison of the 5% damping PSA spectra of the simulated accelerograms as obtained by Methods I and II. It is clear from the figure that the two spectra are fairly close to each other.

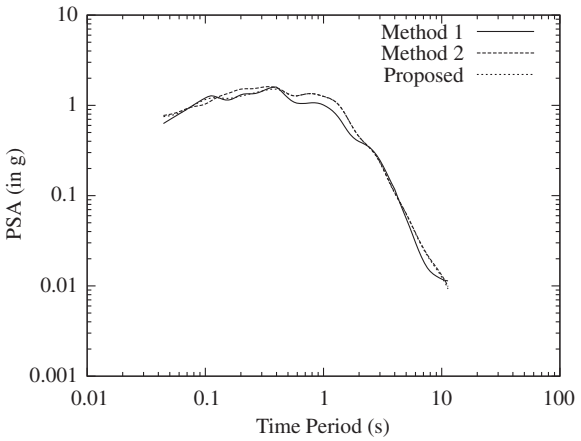

Figure 1. Comparison of PSA spectra for Method I, Method II, and the proposed hybrid method in the case of Aftershock 2352 at Station N042.

DOI: 10.1002/eqe

At very long periods, however, the spectrum for Method I appears to be having an unrealistic rate of decay with increase in period, possibly due to the problems with the estimation of $\alpha(T)$ at very long periods as discussed above.

Figure 2 shows a similar comparison for Aftershock 1757 (occurrence at 17:57 h on September 20, 1999; $M_L = 6.44$) recorded at Station H006 along the EW direction. Here also, the PSA spectra of the simulated aftershock accelerograms by the two methods are in very good agreement except for very stiff oscillators. In this case, Method II appears to give an accelerogram with unusually high PSA ordinates at short periods, possibly due to the unrealistic β_j values at lower j's as shown in the variation of β_j with level j in Figure 3. The values of β_j shown in Figure 3 work satisfactorily, despite being unrealistically high at small j values, for the modification of

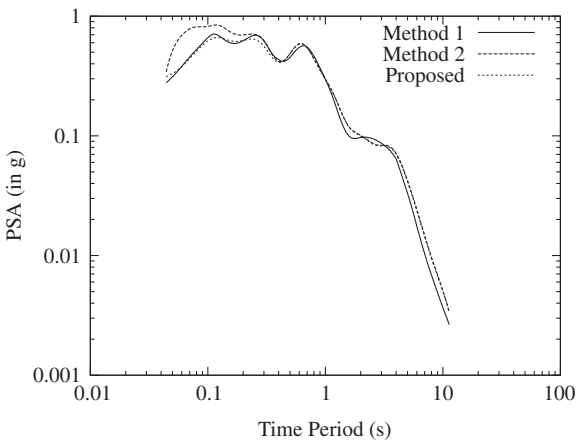

Figure 2. Comparison of PSA spectra for Method I, Method II, and the proposed hybrid method in the case of Aftershock 1757 at Station H006.

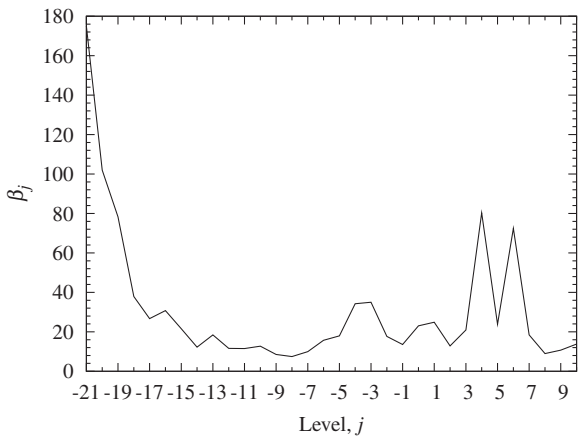

Figure 3. Scale factor β_j for modification of the main shock accelerogram recorded at Station H006 along the EW direction.

DOI: 10.1002/eqe

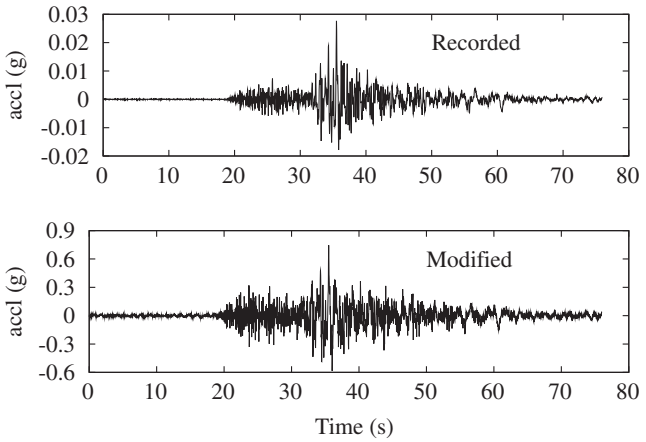

Figure 4. Modified and recorded accelerograms in the case of aftershock recorded at Station N042.

the recorded main shock accelerogram. However, it is clear that those fail to modify the recorded aftershock accelerogram satisfactorily at short periods.

It is obvious from the above that Methods I and II are suitable, respectively, for shorter and longer periods. In the intermediate periods, both give comparable results. Hence, a hybrid method combining both Methods I and II is proposed. In this method, Method II is employed first as discussed above and β_j's are obtained. This is followed by iterative modification of β_j's for those period bands that are on the left of the period of the dominant peak in the $\mathrm{DS}_{\mathrm{Aft}}(T)$ spectrum such that the PSA values of the modified accelerogram become consistent with the $\mathrm{DS}_{\mathrm{Aft}}(T)$ spectrum at those period bands. The β_j values for the other period bands remain unchanged in this process, and therefore the PSA values at the corresponding periods come out to be almost the same as those in the case of Method II. The 5% damping PSA spectra for the modified accelerograms, as obtained via the hybrid method, for the Aftershocks 2352 and 1757 are shown in Figures 1 and 2, respectively. Figures 4 and 5 show the recorded and modified accelerograms, respectively, for the Aftershocks 2352 and 1757. It may be observed from these figures that the hybrid method gives simulated accelerograms that look realistic and have PSA spectra that overcome the limitations of Methods I and II.

4. SYNTHESIS WITHOUT RECORDED AFTERSHOCK MOTION

This section considers the development of an algorithm for those situations where the recorded aftershock motion is not available, whereas the PSA spectrum and duration of the motion to be simulated are available instead. It is assumed that the main shock accelerogram recorded at the same or a similar site and the (design) PSA spectrum for the (anticipated) main shock that would precede the aftershock motion to be simulated continue to be available.

The algorithm to be proposed here is based on shrinking in length the simulated accelerogram for the anticipated main shock motion, assuming that the pattern of arrival of different seismic waves for an aftershock motion is similar to that in the main shock motion. Shrinking of an

DOI: 10.1002/eqe

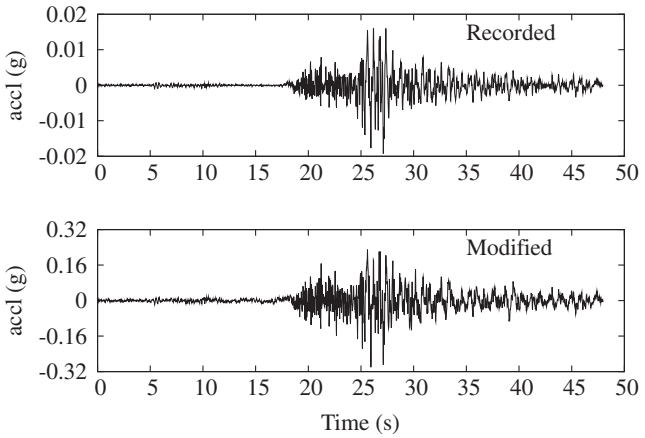

Figure 5. Modified and recorded accelerograms in the case of aftershock recorded at Station H006.

accelerogram, without affecting its frequency content, can be done conveniently by modelling of the wavelet coefficients of the accelerogram as proposed by Basu and Gupta [11].

The wavelet coefficient $W_\psi f(a_j, b)$ of a realization $f(t)$ of a ground acceleration process corresponding to the jth level may be approximated by a harmonic function that has the predominant central frequency

$$\omega_{1j} = \frac{(\sigma+1)\pi}{2a_j} \tag{13}$$

and is modulated by (i) a slowly varying harmonic function with the frequency

$$\omega_{2j} = \frac{(\sigma-1)\pi}{2a_j} \tag{14}$$

and (ii) by a realization of a (time-varying) random amplitude envelope process, $V_j(b)$. $W_\psi f(a_j, b)$ is thus represented as [11]

$$W_\psi f(a_j, b) = V_j(b) \sin(\omega_{2j} b + \phi_{2j}) \sin(\omega_{1j} b + \phi_{1j}) \tag{15}$$

Here, ϕ_{1j} and ϕ_{2j} are statistically independent, uniformly distributed random variables over $[0, 2\pi]$. For a given realization, $V_j(b)$ and ϕ_{1j} are known *a priori*, and therefore, $W_\psi f(a_j, b)$ may be expressed as

$$W_\psi f(a_j, b) = U_j(b) \sin(\omega_{1j} b + \phi_{1j}) \tag{16}$$

where $U_j(b)$ is the level-wise envelope function. This may be obtained in case of a realization, for the level j, by joining the positive peaks in the variation of $W_\psi f(a_j, b)$ of the realization with b. It is not necessary to determine ϕ_{1j} as we are interested only in modelling the realization using its salient temporal features.

Let us say that $f(t)$ represents the anticipated main shock accelerogram that has been obtained using modification of the given recorded accelerogram (for compatibility with the target PSA spectrum), and that the envelope function $U_j(b)$ has been obtained for all levels. The shape of this

DOI: 10.1002/eqe

function for a level j describes the arrival pattern of energy in the waves in the frequency band corresponding to the level j. In the absence of any other known linkage between the main shock and aftershock motions, it is assumed here that the identical pattern of energy arrival will hold good for various aftershocks to be recorded at the same station. This appears reasonable as long as the mechanism of energy release at source during the aftershock can be assumed to be similar to that during the main shock. Considering that the main shocks result from tens or hundreds of kilometers fault ruptures as against aftershocks that are associated with smaller faults resulting in simpler rupture mechanisms, this assumption may not usually hold good. The impact of this assumption will therefore be examined later through a numerical study.

Keeping the shape of the envelope function unchanged at all levels, the main shock accelerogram may be shrunk by a shrink factor k (usually $k<1$; $k>1$ implies stretching) and the wavelet coefficient $W_\psi f(a_j, b)$ may be modified to $\bar{W}_\psi f(a_j, b)$ such that

$$\bar{W}_\psi f(a_j, b) = U_j(\bar{b}) \sin(\omega_{1j} b + \phi_{1j}) \tag{17}$$

with $\bar{b} = b/k$. It may be noted that the effect of the shrink factor is uniformly incorporated in all envelope functions and that the predominant central frequencies of $\bar{W}_\psi f(a_j, b)$ and $W_\psi f(a_j, b)$ continue to be identical. The shrink factor is proposed to be the same as the ratio of the target strong motion duration (of the aftershock accelerogram to be simulated) to the (actual) strong motion duration of the corresponding main shock accelerogram. In this study, strong motion duration of the main shock accelerogram is assumed to be obtained by using the definition proposed by Trifunac and Brady [6]. In order to illustrate the proposed shrinking using the shrink factor k, we consider the recorded EW component of the main shock motion at Station H006. Figure 6 shows the (actual) wavelet coefficients $W_\psi f(a_j, b)$ for the original motion and the (modelled) wavelet coefficients $\bar{W}_\psi f(a_j, b)$ for the shrunk motion with $k = 0.5$, in the case of $j = -6$ and ϕ_{1j} assumed arbitrarily. It may be observed that the shape of the envelope function and the frequency content of the original motion remain unchanged in the shrunk motion. Figure 7 shows a comparison of the normalized Fourier spectra of the recorded accelerogram and the shrunk accelerogram. The two spectra are in good agreement even though some discrepancies exist, possibly due to the imperfect modelling of the wavelet coefficients using Equation (16).

The accelerogram reconstructed from $\bar{W}_\psi f(a_j, b)$ will need to be modified further for compatibility with the target PSA spectrum of the aftershock, e.g. by using the procedure of Mukherjee and Gupta [9]. However, before modification, it is necessary to ensure that the ratio of the strong motion duration of the reconstructed accelerogram to its total duration is not too small. It has been observed by comparing several main shock records with the corresponding aftershock records that main shock records are usually associated with much longer tails compared with the aftershock records. In case of aftershock records, therefore, this ratio usually stays above 0.25. In view of this, it is proposed to curtail the tail of the reconstructed accelerogram and make this ratio equal to 0.25, in case it falls below 0.25.

Thus, the proposed algorithm may be summarized in the following steps: (i) modification of the recorded main shock accelerogram for compatibility with the target PSA spectrum of the anticipated main shock; (ii) determination of the strong motion duration for the simulated main shock accelerogram and calculation of the shrink factor k by using the target strong motion duration of the aftershock motion to be simulated; (iii) calculation of the wavelet coefficients of the simulated main shock accelerogram and their modelling as in Equation (16); (iv) modification of the calculated wavelet coefficients as in Equation (17) by using the shrink factor k; (v) reconstruction of the

DOI: 10.1002/eqe

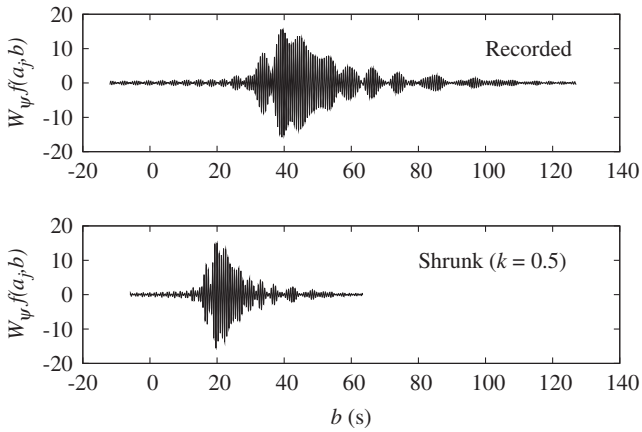

Figure 6. Comparison of wavelet coefficients for level $j=-6$ in the cases of recorded and shrunk accelerograms.

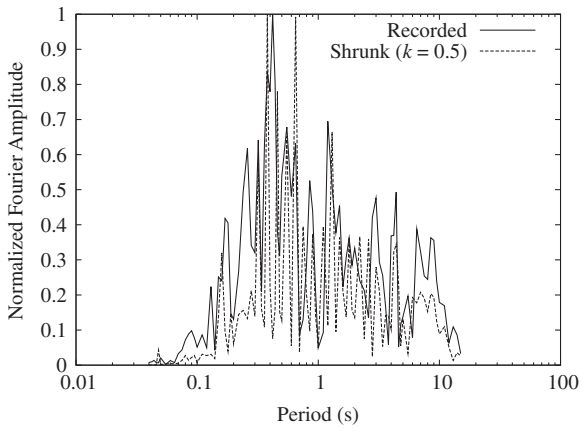

Figure 7. Comparison of normalized Fourier amplitude spectra for the recorded and shrunk accelerograms.

aftershock accelerogram from the modified wavelet coefficients, $\bar{W}_\psi f(a_j, b)$; (vi) curtailment of the reconstructed accelerogram at its tail, if necessary; and (vii) modification of the reconstructed accelerogram for compatibility with the target PSA spectrum of the anticipated aftershock.

To illustrate the proposed algorithm, the main shock and Aftershock 0014 (occurrence at 00:14 h on September 22, 1999; $M_L = 6.8$) of the Chi–Chi 1999 earthquake recorded at Station N041 along the EW direction are considered. The main shock accelerogram is shrunk by using a factor of 0.367, which is the ratio of the strong motion duration of the recorded aftershock accelerogram to the strong motion duration of the main shock accelerogram, and then the shrunk accelerogram is modified to match the PSA spectrum of the recorded aftershock accelerogram by using the procedure of Mukherjee and Gupta [9]. The simulated aftershock accelerogram is compared with

DOI: 10.1002/eqe

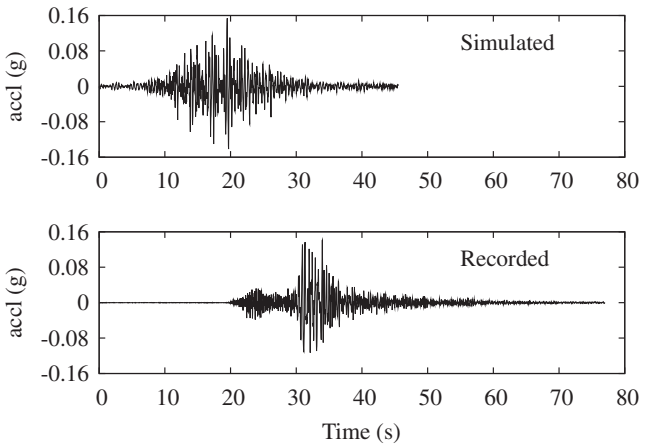

Figure 8. Comparison between recorded and simulated aftershock accelerograms in the case of Station N041 record.

the recorded aftershock accelerogram in Figure 8. It is apparent from the figure that even though the recorded and simulated accelerograms look comparable in strong motion duration, both look different in terms of the arrival of different waves. This may indeed be the situation in many a cases because there is no physical basis to assume that the aftershock motion would follow the same arrival pattern of waves as that followed by the main shock motion. However, such an assumption may be reasonable as a first step in the simulation of aftershock accelerograms when appropriate aftershock records are not available. Further, since one of the important applications of the simulated accelerograms is in the non-linear time-history analyses of structural systems, it will be interesting to see whether despite the observed disagreement, the simulated accelerogram is consistent with the recorded accelerogram in terms of non-linear response and damage.

For estimating the non-linear response, a series of elastic–perfectly plastic oscillators with initial period T ranging from 0.044 to 4 s and with F-damping of 5% are considered. All oscillators have different yield force levels, and the yield level for an oscillator is chosen so that the maximum displacement response is four times the yield displacement in response to the simulated accelerogram. These oscillators are subjected to the recorded and simulated aftershock accelerograms, and maximum non-linear displacement SD(T) spectrum and hysteresis energy EH(T) spectrum are compared for the two ground motions. These two response parameters are specifically chosen as it is quite common to define damage as a linear combination of these parameters, and thus, agreement (between the simulated and recorded accelerograms) in terms of these parameters would ensure agreement in terms of damage as well. Figure 9 shows a comparison of the normalized SD(T) and EH(T) spectra as obtained from the recorded and simulated accelerograms (see Figure 8). The curves with symbols correspond to EH(T) and those without symbols to SD(T). The curves in solid lines correspond to the recorded accelerogram and those in dashed lines to the simulated accelerogram. It is obvious from the figure that the simulated accelerogram is reasonably consistent with the recorded accelerogram in terms of both non-linear spectral displacement and hysteresis energy dissipation.

Figure 10 shows another set of recorded and simulated accelerograms. The recorded accelerograms in this case pertain to Station I013 and the EW direction, and the shrink factor k here

DOI: 10.1002/eqe

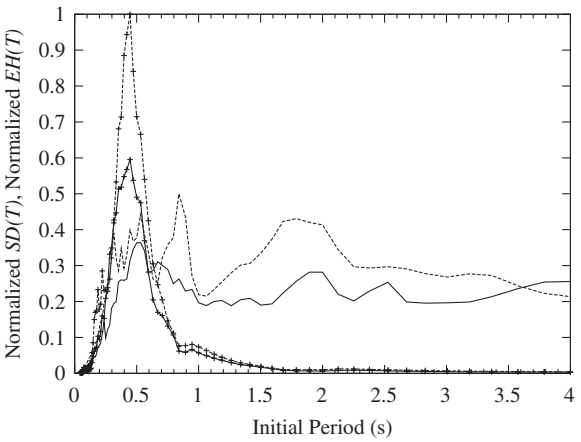

Figure 9. Comparison between SD(T) and EH(T) spectra for recorded and simulated aftershock motions in the case of N041 Station record (curves without symbols correspond to SD(T) and with symbols to EH(T); solid lines correspond to recorded motions and dashed lines to simulated motions).

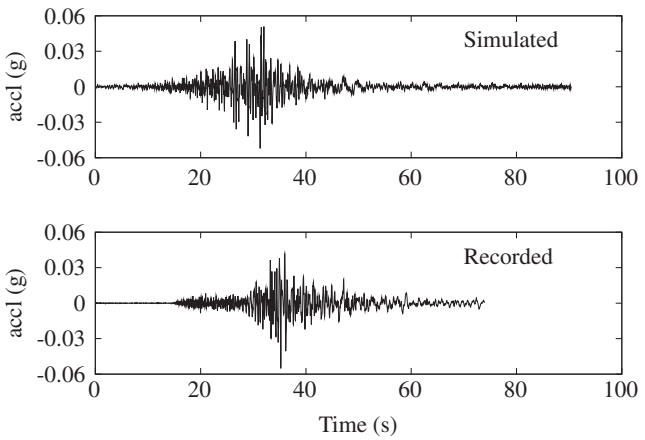

Figure 10. Comparison between recorded and simulated aftershock accelerograms in the case of Station I013 record.

is 0.772. The recorded and simulated accelerograms appear to be much more similar in this case, clearly due to the similarity between the recorded main shock and aftershock motions. Figure 11 shows the comparison in terms of SD(T) and EH(T), and it is clear that the simulated motion can be a good replacement for the recorded motion in this example.

It is clear from the two example cases considered so far and many more such examples that the recorded and simulated accelerograms would lead to reasonable consistency in terms of non-linear response and damage as long as the two are consistent in terms of strong motion duration and PSA spectrum. This is irrespective of whether the assumption of motion during the aftershock following the same wave arrival pattern as that during the main shock is violated or not. We now

DOI: 10.1002/eqe

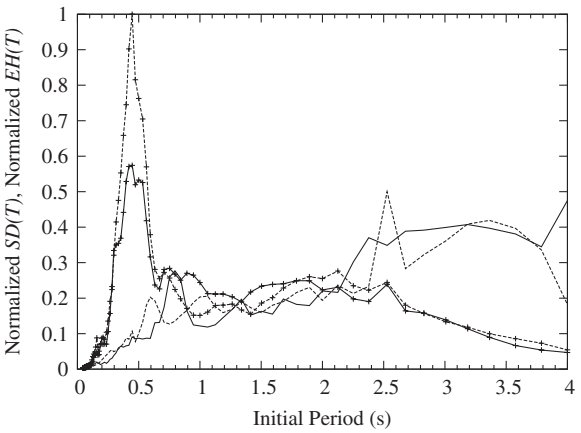

Figure 11. Comparison between SD(T) and EH(T) spectra for recorded and simulated aftershock motions in the case of I013 Station record (curves without symbols correspond to SD(T) and with symbols to EH(T); solid lines correspond to recorded motions and dashed lines to simulated motions).

consider another case where the strong motion parts of the simulated and recorded motions are significantly different. Figure 12 shows the comparison between the recorded and simulated aftershock accelerograms in the case of Aftershock 2352 (occurrence at 23:52 h on September 25, 1999; $M_L = 6.8$) recorded at Station C029 along the EW direction. In this case, besides no visual similarity, both recorded and simulated motions do not even have comparable lengths of strong motion segments. As a result, very poor agreement is seen between the hysteresis energy dissipation for the two motions (see Figure 13). Compatibility between the maximum (non-linear) displacement responses is somewhat ensured due to the forced (elastic) PSA spectra compatibility in the proposed algorithm. This kind of situation where the proposed algorithm does not work properly may develop when the definition of duration used fails to identify the stationary segment correctly in the main shock motion.

Figure 14 shows the recorded and simulated accelerograms for a case (Aftershock 2352, Station T109, EW direction) where the strong motion segment of the recorded aftershock includes a significant gap in between the two different pulses of energy arrival, whereas such a feature is missing in the recorded main shock. As a result, the simulated accelerogram gets a much longer stationary segment ($k = 1.9$) compared with the recorded main shock. As seen in Figure 14, the strong motion segments in the recorded and simulated accelerograms are clearly inconsistent, and therefore the proposed algorithm would not work properly. Figure 15 shows that the EH(T) spectrum for the simulated accelerogram is consistently higher than that for the recorded accelerogram.

5. CONCLUSIONS

In this study, algorithms have been proposed for the simulation of aftershock accelerograms for two scenarios. In the first scenario, the simulated accelerogram is made consistent with a recorded aftershock accelerogram in terms of temporal features. It is also made consistent with the (design) PSA spectrum of the (anticipated) main shock that would precede the aftershock. It is assumed that

DOI: 10.1002/eqe

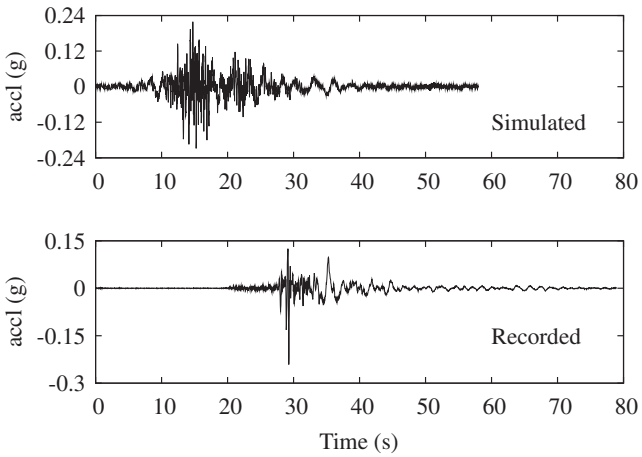

Figure 12. Comparison between recorded and simulated aftershock accelerograms in the case of Station C029 record.

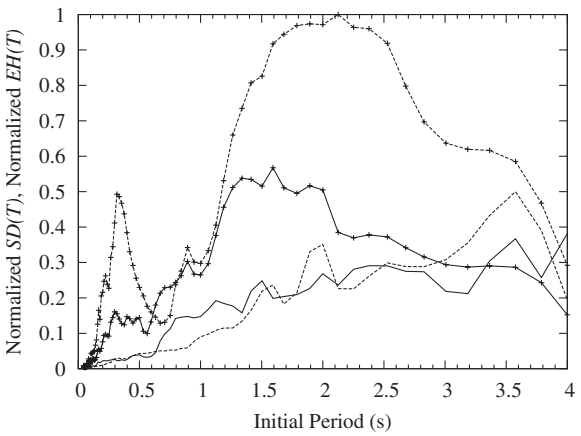

Figure 13. Comparison between SD(T) and EH(T) spectra for recorded and simulated aftershock motions in the case of C029 Station record (curves without symbols correspond to SD(T) and with symbols to EH(T); solid lines correspond to recorded motions and dashed lines to simulated motions).

the recorded main shock accelerogram is available for the station to which the recorded aftershock accelerogram corresponds. The recorded aftershock accelerogram is proposed to be modified by using a hybrid method wherein for short periods, the simulated accelerogram is made consistent with the aftershock PSA spectrum estimated from the main shock PSA spectrum. For long periods, it is assumed that same modifications would apply on the recorded aftershock accelerogram as in modifying the (recorded) main shock motion to match with the design spectrum.

In the second scenario, the target aftershock accelerogram is not available. Instead, estimates of the PSA spectrum and strong motion duration of the aftershock motion to be simulated are assumed to be available. The proposed algorithm works on the assumption that the temporal features of the

DOI: 10.1002/eqe

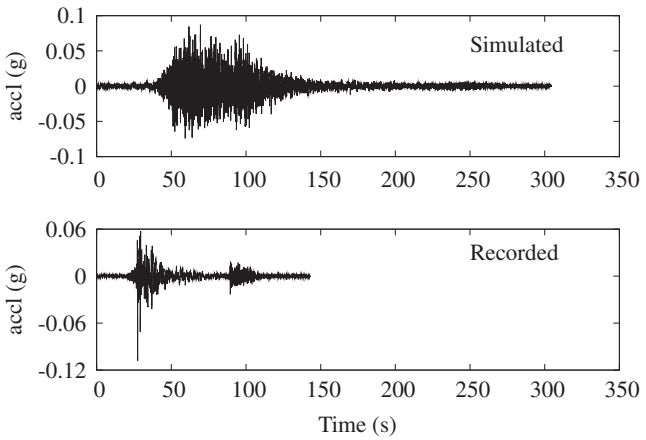

Figure 14. Comparison between recorded and simulated aftershock accelerograms in the case of Station T109 record.

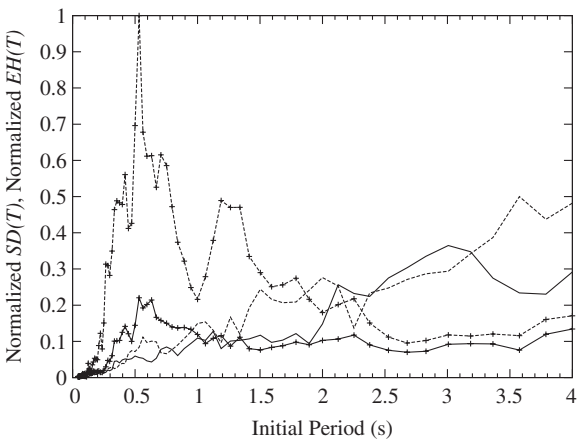

Figure 15. Comparison between SD(T) and EH(T) spectra for recorded and simulated aftershock motions in the case of T109 Station record (curves without symbols correspond to SD(T) and with symbols to EH(T); solid lines correspond to recorded motions and dashed lines to simulated motions).

main shock motion get replicated on a reduced scale in the aftershock motions. This assumption is unrealistic and may not always work. Through numerical examples, however, it has been shown that this may not be a serious limitation, provided we have good estimate of the factor by which the strong motion segment in the main shock motion gets shrunk to the strong motion segment of the aftershock motion. In that case, the simulated aftershock accelerograms would lead to a reasonably accurate assessment of the maximum non-linear response and hysteretic energy dissipation in the case of elastic–perfectly plastic oscillators.

It may be noted that the algorithm proposed for the second scenario is critically dependent on the estimation of the PSA spectrum and strong motion duration of the anticipated aftershock motion.

DOI: 10.1002/eqe

Statistical analyses therefore need to be carried out to establish correlations of the PSA spectra and strong motion durations of aftershocks with the PSA spectra and strong motion durations of main shocks. This aspect will be dealt with in another paper by the authors.

ACKNOWLEDGEMENTS

The authors are grateful to Dr Chien-Fu Wu of Seismology Center of Central Weather Bureau, Taipei, Taiwan for making the recorded data for the Chi–Chi earthquake and its aftershocks available for this study.

REFERENCES

1. Gupta VK, Nielsen SRK, Kirkegaard PH. A preliminary prediction of seismic damage-based degradation in RC structures. *Earthquake Engineering and Structural Dynamics* 2001; **30**:981–993.
2. Hancock J, Watson-Lamprey J, Abrahamson NA, Bommer JJ, Markatis A, McCoy E, Mendis R. An improved method of matching response spectra of recorded earthquake ground motion using wavelets. *Journal of Earthquake Engineering* 2006; **10**(1):67–89.
3. Johnson RA. An earthquake spectrum prediction technique. *Bulletin of the Seismological Society of America* 1973; **63**(4):1255–1274.
4. McGuire RK. Seismic design spectra and mapping procedures using hazard analysis based directly on oscillator response. *Earthquake Engineering and Structural Dynamics* 1977; **5**:211–234.
5. Kamiyama M, Yanagisawa E. A statistical model for estimating response spectra of strong earthquake ground motions with emphasis on local soil conditions. *Soils and Foundations* 1986; **26**(2):16–32.
6. Trifunac MD, Brady AG. A study on the duration of strong earthquake ground motion. *Bulletin of the Seismological Society of America* 1975; **65**:581–626.
7. Basu B, Gupta VK. Seismic response of SDOF systems by wavelet modelling of nonstationary processes. *Journal of Engineering Mechanics* (ASCE) 1998; **124**(10):1142–1150.
8. Daubechies I. *Ten Lectures on Wavelets*. Society for Industrial and Applied Mathematics: Philadelphia, PA, U.S.A., 1992.
9. Mukherjee S, Gupta VK. Wavelet-based generation of spectrum-compatible time-histories. *Soil Dynamics and Earthquake Engineering* 2002; **22**:799–804.
10. USNRC. *Design Response Spectra for Seismic Design of Nuclear Power Plants*, *Regulatory Guide 1.60*. United States Nuclear Regulatory Commission, 1973.
11. Basu B, Gupta VK. Stochastic seismic response of single-degree-of-freedom systems through wavelets. *Engineering Structures* 2000; **22**:1714–1722.

DOI: 10.1002/eqe